Noureddine Leguedani, My Mustapha Hafid,
Siham Yazami el Idrissi, and Yousra kessad

Impedance study of Ni-Cr alloy in contact with biologic and organic solution using constant phase element

Abstract: The electrochemical characterization of the Ni-Cr dental implant alloy was studied by electrochemical impedance spectroscopy (EIS) in contact with artificial saliva, milk and vinegar. For all solutions the data impedance has been recorded maintaining the sample at 37°C for 1 hour of immersion. In this chapter we are focused on the modeling of the response function of this biomaterial using an equivalent electric circuit (EEC). The experimental results show that the Ni-Cr alloy exhibits a quite good resistance to corrosion, with passive properties referring to the existence of a thick passive film. An EEC was proposed to describe the electrochemical behavior of this biomaterial in the frequency range of 0–40 kHz. The Bode diagram indicates the presence of at least one time constant during the kinetic process. The nature of the film and the morphology of the interface biomaterial/film/electrolyte are presented in this chapter. The proposed circuit involved constant phase elements in order to explain the apparent heterogeneity on the interface biomaterial/film/electrolyte. Simulation based on this model showed a good agreement with the experimental data, with a best fit corresponding to a minimum standard deviation (the chi-square value χ^2 is 10^{-4}).

Keywords: Ni-Cr, biomaterial, electrochemical impedance spectroscopy (EIS), electrical equivalent circuit (EEC), constant phase element (CPE), interface biomaterial/film/electrolyte

1 Introduction

Ni-Cr-based alloys are part of materials used on orthodontics as dental prostheses. Their study has become easier owing to their lower cost, by their biocompatibility and by the existence of a variety of software able to fit the data impedance. The Ni-Cr alloys are commonly used for dental materials [1] and widely used in dental skeletal structures, implant fixtures and prosthodontic restoration [2]. Beside their low cost they exhibit acceptable mechanical and tribological properties and matching thermal expansion coefficient with the ceramics of metal–ceramic restorations [3, 4]. There also known as passive system with a spontaneous formation of thin passive oxide film

Noureddine Leguedani, My Mustapha Hafid, Siham Yazami el Idrissi, Yousra kessad, Laboratory of Engineering Physics and Environment, Department of Physics, Faculty of Science, University Ibn Tofail, Kenitra, Morocco, e-mail: leguedani@yahoo.fr

https://doi.org/10.1515/9783110558920-006

on the interface metal/electrolyte [5]. The reactivity of the oxide superficial layer formation, which is based especially on Cr_2O_3, will be investigated by electrochemical impedance spectroscopy (EIS). Moreover, we study the reactivity of the superficial oxide layer while varying the solution (pH). We used three solutions, namely, artificial saliva (pH ≈ 6.8), milk (pH ≈ 6.5 to 6.7) and vinegar (pH ≈ 3), to evidence the reactivity of the interface. In this work, we compare the Ni-based alloys to the Co-based alloys, with their formed protective film depending highly on the acidity of the solution used [6]. We study by EIS the response of the biomaterials and the reactivity of its passive film, formed with equivalent electric circuit (EEC) involving CPE.

2 Electrochemical characterization

2.1 Impedance spectroscopy measurements

The electrochemical impedance spectroscopy, or also AC impedance, is a non-destructive technique and a useful tool for studying corrosion [7]. This experimental method makes it possible to distinguish the dielectric and electric properties of individual contributions of components [5].

In this method, the sample undergoes a small electronic excitation so its response is pseudo-linear. In a linear (or pseudo-linear) system, the current response (1) and the potential (2) are sinusoidal in the same frequency and shifted in phase.

The sinusoidal perturbation of potential $E(t)$ induces a sinusoidal current $I(t)$; their representations in the polar coordinates is as follows:

$$E(t) = E_0 \sin(\omega t), \tag{1}$$

$$I(t) = I_0 \sin(\omega t + \varphi), \tag{2}$$

where $\omega = 2\pi f$ and E_0 and I_0 are the amplitudes of the potential and the current, respectively.

The impedance of the system (3) can be written following the Ohmic concept as follows:

$$Z(t) = \frac{E(t)}{I(t)} = \frac{E_0 \sin(\omega t)}{I_0 \sin(\omega t + \varphi)} = Z_0 \frac{\sin(\omega t)}{\sin(\omega t + \varphi)}. \tag{3}$$

With Euler's relationship or polar representation of $E(t)$ and $I(t)$, they can be written as follows:

$$E(t) = E_0 e^{(j\omega t)}, \tag{4}$$

$$I(t) = I_0 e^{(\omega t - \varphi)}. \tag{5}$$

The impedance complex (6) of the biomaterials can be rewritten as follows:

$$Z(t) = \frac{E(t)}{I(t)} = Z_0 e^{j\varphi} = Z_0(\cos\varphi + \sin\varphi). \tag{6}$$

The modulus of the complex impedance (7) and the phase angle shift (8) are deduced from the following formulas:

$$|Z(\omega)| = \sqrt{Z_{\text{re}}^2 + Z_{\text{im}}^2}, \tag{7}$$

$$\tan(\varphi) = \frac{Z_{\text{im}}}{Z_{\text{re}}}, \tag{8}$$

where Z_{re} and Z_{im} are the real and imaginary part of the complex impedance, respectively.

The impedance data are profoundly interpreted by much recently developed software. We have used ZSimpwin version 3.10 to fit the response function of the Ni-Cr biomaterial. The EEC consisted of a combination of simple electronic elements (resistance, capacitor and inductance). The numerical simulation must be done with more accuracy to solve difficulties related to the fact that more than one EEC can be able to fit the data.

Studying the response function $Z(\omega)$ we return to interpret two famous diagrams or representations, namely, the diagrams of Bode and Nyquist. There is some literature which talks about the basics of EIS [8–13], and the fields of its applications cover many domains, from biology and medicine to industry. The electrochemical impedance analysis has been performed on the commercial Ni-Cr alloy in the frequency range of 0–40 kHz, after it had been immersed for 1 hour in milk, artificial saliva or vinegar.

2.2 Experimental results

The Bode diagrams (Fig. 1 and Fig. 2) of the Ni-Cr dental alloys recorded in milk, artificial saliva and vinegar show that at least one time constant phase element (CPE) can be distinguished. For artificial saliva and vinegar, the shape of the curves are similar. At high frequencies the absolute impedance curve is almost independent of the frequency, with a phase angle of 0°, and the impedance of the system is reduced to the electrolyte resistance.

For medium frequencies, at 1–100 Hz, a linear frequency dependence of absolute complex impedance with a maximum angle reaching 70°, 65° and 55° for milk, artificial saliva and vinegar, respectively. This range of frequency is marked by the stable film formation.

At low frequencies, the absolute impedance exhibits its high values for milk and artificial saliva, and these values are ten times higher than for vinegar. This difference in the values of the impedance gives an idea of the film formation for the three

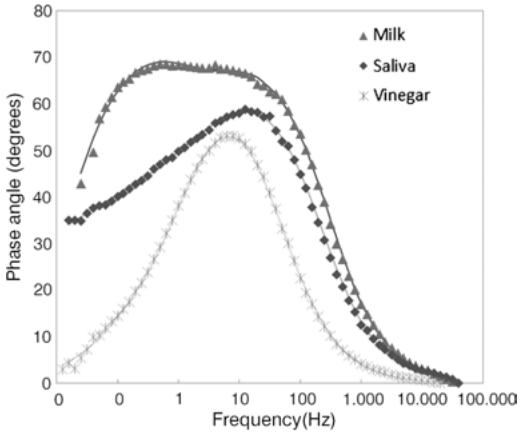

Fig. 1: Phase angle plot for Ni-Cr for milk, saliva and vinegar. The fit based on the model is represented by solid lines.

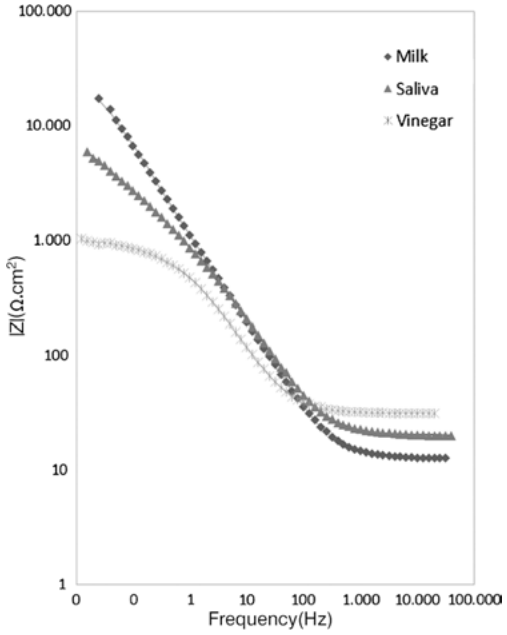

Fig. 2: Measured (discrete points) and fitted (solid lines) values of the *Z* modulus for Ni-Cr dental alloys for milk, saliva and vinegar for 1 hour immersion at 37°C.

solutions under study. This can be explained by the fact that the film is of a porous character in origin. x

The Nyquist plots of Ni-Cr dental alloys are shown in Fig. 3 for the three solutions (milk, artificial saliva and vinegar) with the potential corrosion E_{corr} and at 37°C. It can be seen from the impedance data that the Ni-Cr implant biomaterial/solution interface exhibits capacitive behavior over a relatively wide frequency region, which is typical for a passive alloy system. The parameters for the solution bulk resistance R_s (experimentally determined by the intersection at high frequency of the Nyquist plot

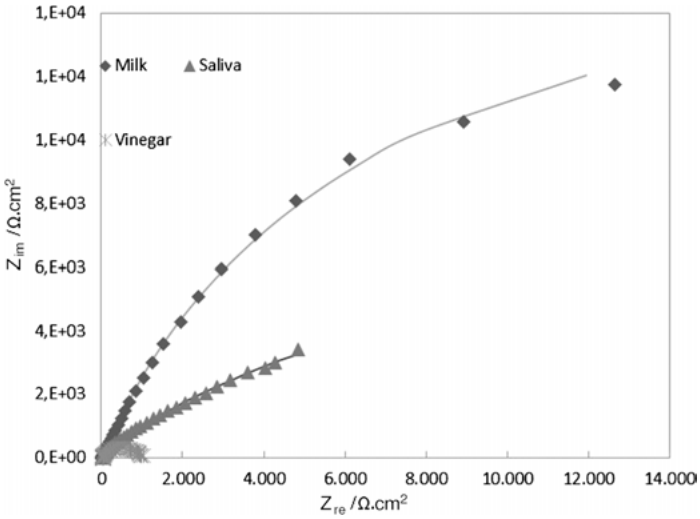

Fig. 3: Nyquist diagram of Ni-Cr dental alloys in the three solutions of milk, artificial saliva and vinegar for 1 hour immersion at 37°C (discrete points).

with the real axis) are of about the same order of magnitude in the three solutions; 12.63 Ω.cm^2 for milk, 19.88 Ω.cm^2 for artificial saliva and 30.9 Ω.cm^2 for vinegar.

The resistance of polarization, R_p (experimentally determined by the diameter of the semi-circles on the arc in the Nyquist plot), related to the corrosion resistance, is found to have high values that increase significantly with milk, artificial saliva and vinegar, respectively.

This high value of R_p implies higher corrosion resistance of implant alloy for milk, reaching a value of 25000 Ω.cm^2, while this value is about 1600 Ω.cm^2 for artificial saliva and 1000 Ω.cm^2 for vinegar.

The low R_p values in vinegar show that the Ni-Cr dental alloys have a weak corrosion resistance when compared to milk and artificial saliva; then a high rate of released metallic ions into the oral environment can take place. The Cole-Cole plot of the complex admittance (Fig. 4) shows the same geometry and the arc dependence of the semi-circle is affected by the nature of the solution used. The diameter of the semi-circle decreases with vinegar, artificial saliva and milk, respectively.

2.3 Modeling the impedance data

The proposed equivalent circuit based on CPE is described in Fig. 5, where R_s is the electrolyte resistance, in series with Q_{out} and in parallel with R_{out}, which is in series with Q_{in}, which is in parallel with R_{in}. Here, Q_{out} denotes the pseudo-capacitance (CPE_{out}) and R_{out} the resistance of the Ni-Cr protection film system, whereas Q_{in} and

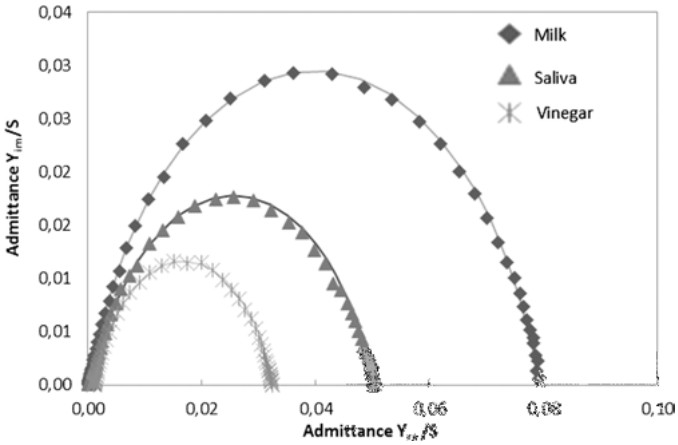

Fig. 4: Admittance diagram of Ni-Cr dental alloys in the three solutions of milk, artificial saliva and vinegar for 1 hour immersion at 37° (discrete points).

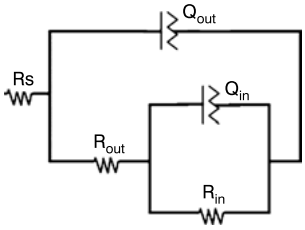

Fig. 5: EEC used in the generation of simulated data.

R_{in} denote the double layer pseudo-capacitance (CPE_{in}) and the transfer resistance of the corrosion of the Ni-Cr/solution interface.

CPE (9) was mathematically used to solve the response of the biomaterial with a non-ideal capacitor interpreting the non-homogeneous behavior of the surface under investigation. The main reasons for adding CPE in a matrix of EEC were the distributed surface reactivity, surface inhomogeneity, roughness and electrode porosity [6]. This lack of homogeneity is modeled with a Q element, used to represent the CPE, i. e.,

$$Z_Q(\omega) = \frac{1}{Y_0(j\omega)^n}, \tag{9}$$

where Y_0 is the admittance of an ideal capacitance and n is an empirical constant, ranging from 0 to 1. The exponent n is related to a non-uniform current distribution due to the surface roughness [7, 8]. It is noteworthy that when $n = 1$, the CPE behaves as a pure capacitor, while when $n = 0$, the CPE behaves as a pure resistor and when $n = 0.5$, the CPE is the equivalent of the so-called Warburg element.

The impedance of ZCPE is defined by $ZCPE_{out} = 1/(j\omega)^{n1}Q_1$ and $ZCPE_{in} = 1/(j\omega)^{n2}Q_2$, where $j^2 = -1$, ω is the angular frequency and the exponents n_1 and n_2 of the CPE_{out}

and CPE_{in} are related to a non-uniform current distribution due to the surface roughness [12]. The chi-square values (χ^2) for all data impedance are of magnitude 10^{-4} indicating an excellent agreement between the experimental data and the model using CPE in the fitting program.

3 Simulation criterion and discussion

Taking into account that several circuits can fit the same data impedance, we aim to determine which of the circuits is more suitable to best describe the corrosion phenomena. We used two criteria to decide which circuits numerically fit the impedance data in search of an optimal configuration. First, only the simple elements introduced into the EEC must have a physical meaning and second, the chi-square value (χ^2) must be less than 10^{-4}. Monitoring numerically the evolution of parameters, one can determine which of the proposed models can be kept. Systematically, the standard deviation in the present work is found to be 1.732×10^{-04} for milk, 3.895×10^{-04} for artificial saliva and 1.693×10^{-04} for vinegar.

From this model it was possible to calculate the polarization resistance, the resistance R_s of the solution, the relaxation frequency of the system and the CPE parameters (the resistance and the capacity of the oxide layer). Thus a simple schematization of the interface (Fig. 6) can be given.

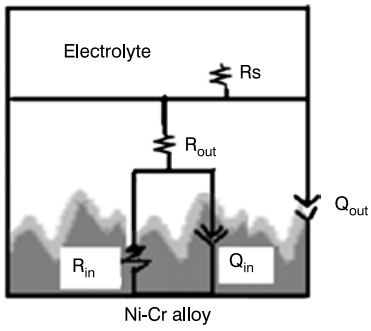

Fig. 6: Modeling of the interface electrode/film/electrolyte of Ni-Cr dental alloys.

Table 1 lists the parameters of the EEC used to simulate the impedance data of the Ni-Cr implant alloy in the presence of milk, artificial saliva and vinegar, maintained at 37°C and for one hour immersion time.

It was found that the values of the resistance of the electrolyte, R_s, for the Ni-Cr implant alloy is increasing with milk (12.63 $\Omega.cm^2$), artificial saliva (20.06 $\Omega.cm^2$) and vinegar (31.06 $\Omega.cm^2$). The resistance of polarization (Fig. 7) is calculated in this model by the sum of R_{in} and R_{out}. The value of R_p decreased; it is 33.588 $k\Omega.cm^2$ for milk, 28.579 $k\Omega.cm^2$ for saliva and 991.2 $\Omega.cm^2$ for vinegar.

Table 1: Model parameters used to simulate the impedance spectra of the Ni-Cr implant alloy in the presence of milk, artificial saliva and vinegar.

	R_s Ω.cm^2	Q_{out} μF.cm^2	n_1	R_{out} Ω.cm^2	Q_{in} μF.cm^2	n_2	R_{in} Ω.cm^2
Vinegar	31.06	313.6	0.82	715.5	3734	0.72	275.7
Milk	12.63	171.9	0.82	2848	35.5	0.89	3.07×10^{04}
Saliva	20.06	163.5	0.8	699	380.4	0.44	2.79×10^{4}

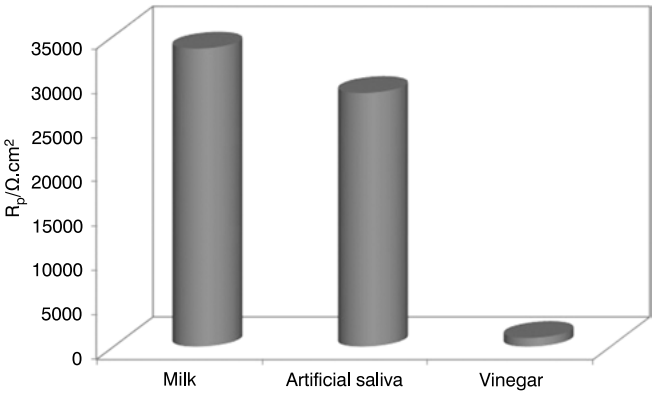

Fig. 7: Resistance of polarization, R_p, of Ni-Cr alloys in the three solutions of milk, artificial saliva and vinegar.

The theoretical model predictions are in good agreement with the experimental data. Thus, the Q_{out} capacitance values in all solutions were within a range of 172–314 μF.cm^2, with n within a range of 0.8029–0.8213, which indicates a non-ideal capacitance interface (so an oxide passive layer exists).

Moreover, the Q_{in} capacitance values are highly dependent on milk, artificial saliva and especially of vinegar; the values of n have the same order in milk (0.8924) and in vinegar (0.7151), but not in saliva, which shows a value of 0.4361.

4 Conclusion

The corrosion interface of Ni-Cr alloys in biological (milk and artificial saliva) and organic solutions (vinegar) was studied by EIS based on a model using CPE. Results show that this biomaterial exhibits a good corrosion resistance in milk and artificial saliva and a weak corrosion resistance in vinegar. All the n values in the three solutions were found to be within a range of 0.7151 to 0.8924, indicating that the corrosion interface deviated from a pure ideal capacitor. The phase angle maximum (φ_{max}) in this

biomaterial is measured at approximately –53 to –70 degrees. The EEC predictions are in good agreement with the experimental data.

Bibliography

[1] K. F. Leinfelder, "An evaluation of casting alloys used for restorative procedures", The Journal of the American Dental Association, vol. 128, pp. 37–45, 1997.
[2] H.-S. Kima, M.-K. Sonb, and H.-C. Choec, Journal of the Korean Institute of Surface Engineering, vol. 49, no. 3, 2016.
[3] J. C. Wataha, N. L. O'Dell NL, B. B. Singh, M. Ghazi, G. M. Whitford, and P. E. Lockwood, "Relating nickel-induced tissue inflammation to nickel release in vivo", Journal of Biomedical Materials Research, vol. 58, pp. 537–544, 2001.
[4] R. M. Joias, R. N. Tango, J. E. Junho de Araujo, M. A. Junho de Araujo, Gde S. Ferreira Anzaloni Saavedra, T. J. Paes-Junior, and E. T. Kimpara, "Shear bond strength of a ceramic to Co-Cr alloys", The Journal of Prosthetic Dentistry, vol. 99 pp. 54–59, 2008.
[5] H. Cesiulis, N. Tsyntsaru, A. Ramanavicius, and G. Ragoisha, "Nanostructures and thin films for multifunctional applications", NanoScience and Technology, pp. 3–42, April 2016.
[6] A. Ouerd, C. Alemany-Dumont, B. Normand, and S. Szunerits, Electrochimica Acta, vol. 53, pp. 4461–4469, 2008.
[7] A. S. Hamdy, E. El-Shenawy, and T. El-Bitar, International Journal of Electrochemical Science, vol. 1, pp. 171–180, 2006.
[8] M. Sluyters-Rehbah, "Impedances of electrochemical systems: terminology, nomenclature and representation. Part 1. Cells with metal electrodes and liquid solutions". Pure and Applied Chemistry, vol. 66, no. 9, pp. 1831–1891, 1994.
[9] A. J. Bard and L. R. Faulkner, "Electrochemical Methods. Fundamentals and Applications", Wiley, New York, 2001, 829 pp.
[10] E. Barsoukov and J. R. Macdonald (eds.), "Impedance Spectroscopy Theory, Experiment, and Applications", Wiley, New York, 2005, 595 pp.
[11] M. E. Orazem and B. Tribollet, "Electrochemical Impedance Spectroscopy", Wiley, New York, 2008, 523 pp.
[12] A Lasia, In: "Electrochemical Impedance Spectroscopy and its Applications", ed. by B. E. Conway, J. O'M. Bockris, R. E. White, Modern Aspects of Electrochemistry, vol. 32, Kluwer Academic Publishers, New York, pp. 143–248.
[13] A. Lasia, "Electrochemical Impedance Spectroscopy and its Applications", Springer, New York, 2014, 367 pp.